The final publication is available at

https://doi.org/10.1111/jce.15311

Additional Information

Relationship between luminal esophageal temperature and volume of esophageal injury during RF ablation:

In silico study comparing low power-moderate duration vs. high power-short duration

Juan J. Pérez, MSc, PhD, [1] Ana González-Suárez, MSc, PhD, [2,3] Timothy Maher, MD,[4]

Hiroshi Nakagawa, MD, PhD,[5] Andre d'Avila, MD, PhD, [4] Enrique Berjano, MSc, PhD[1]

From [1] BioMIT, Department of Electronic Engineering, Universitat Politècnica de València, Valencia, Spain, [2] Electrical and Electronic Engineering, National University of Ireland Galway, Ireland, [3] Translational Medical Device Lab, National University of Ireland Galway, Ireland, [4] Division of Cardiovascular Medicine, Beth Israel Deaconess Medical Center, Harvard Medical School, Boston, MA, USA, [5] Department of Cardiovascular Medicine, Cleveland Clinic, Cleveland, OH, USA

Corresponding author: Enrique Berjano, Department of Electronic Engineering (Building 7F), Universitat Politècnica de València, Camino de Vera, 46022 Valencia, Spain. Email: eberjano@eln.upv.es

Word count: 4,338
Running head: Esophageal damage during RF ablation

The authors have no conflicts to disclose.

Data availability: The data underlying this article will be shared on reasonable request to the

corresponding author.

Abstract

OBJECTIVE: To model the evolution of peak temperature and volume of damaged esophagus during and after RF ablation using low power-moderate duration (LPMD) vs. high power-short duration (HPSD) or very high power-very short duration (VHPVSD) settings.

METHODS: An *in silico* simulation model of RF ablation accounting for left atrial wall thickness, nearby organs and tissues, as well as catheter contact force. The model used the Arrhenius equation to derive a thermal damage model and estimate the volume of esophageal damage over time during and after RF application under conditions of LPMD (30W, 20s), HPSD (50W, 6s), and VHPVSD (90W, 4s).

RESULTS: There was a close correlation between maximum peak temperature after RF application and volume of esophageal damage, with highest correlation ($R^2 = 0.97$) and highest volume of esophageal injury in the LPMD group. A greater increase in peak temperature and greater relative increase in esophageal injury volume in the HPSD (240%) and VHPVSD (270%) simulations occurred after RF termination. Increased endocardial to esophageal thickness was associated with a longer time to maximum peak temperature ($R^2 > 0.92$), especially in the HPSD/VHPVSD simulations, and no esophageal injury was seen when the distances were > 4.5 mm for LPMD or > 3.5 mm for HPSD.

CONCLUSION: LPMD is associated with a larger total volume of esophageal damage due to the greater total RF energy delivery. HPSD and VHPVSD shows significant thermal latency (resulting from conductive tissue heating after RF termination), suggesting a requirement for fewer esophageal temperature cutoffs during ablation.

1. Introduction

Esophageal injury during radiofrequency catheter ablation (RFCA) for atrial fibrillation can lead to atrioesophageal fistulas which are rare but potentially lethal complications which caused by radiofrequency (RF) energy transfer from the posterior wall of the left atrium to the esophagus. Esophageal temperature monitoring via a probe placed in the lumen of the esophagus is commonly used to reduce the risk of esophageal injury by alerting the operator of esophageal heating and prompting discontinuation of ablation in that location. It has been observed both *in vivo* and with computer modeling that RF lesions can continue to grow deeper even after the termination of RF application due to conductive heating, which results in delayed tissue heating, termed thermal latency.[1,2] Commercial luminal esophageal temperature monitors may detect thermal latency at different rates, although newer technologies using high resolution infrared thermal imaging can rapidly and accurately measure peak esophageal temperature and predict post-ablation esophageal injuries.[3]

To reduce lesion depth, and therefore reduce esophageal injury during RFCA, ablating with higher power for shorter impulse durations (HPSD; use of 50 W for < 10 seconds) is often employed.[4,5] The proposed benefit of HPSD is that it employs primarily electrical resistive heating as opposed to the thermal conductive heating observed in longer RF applications, and thus limiting delayed lesion depth growth.[6] However, computer modeling data has previously demonstrated significant thermal latency leading to late lesion growth during HPSD RF ablation, and observational data from RFCA for atrial fibrillation with HPSD has not shown a reduction in

3

esophageal lesions.[2,7] It is not well known how traditional ablation parameters differ from higher

powers with shorter ablation durations in terms of thermal latency and peak temperatures

achieved and how that relates to the amount of esophageal injury. In this study, we sought to use

computer modeling to simulate the esophageal thermal dynamics during and after RFCA under

three different power settings: low power-moderate duration (LPMD, 25 W−20 s), high power-

short duration (HPSD, 50 W−6 s) and very high power-very short duration (VHPVSD, 90 W−4

s).

2. Methods

2.1. Model description

A three-dimensional computational model was built including the atrial wall thickness values of

1.0, 1.5 and 2.0 mm, epicardial fat layer of 0 (i.e. no fat layer), 0.5 and 1.0 mm, blood inside the

atrium, esophagus, aorta, lungs and surrounding connective tissue between the endocardium and

the outer esophageal surface of 2.5 to 6.5 mm.[7–9] We modeled a 7Fr 3.5 mm irrigated electrode

perpendicular to the atrial wall. Irrigation was modeled by fixing a value of 45 ºC in the

cylindrical zone of the electrode tip, and leaving the semispherical tip free (as described in Pérez

et al[10]) which mimics a multi-hole electrode since we are assuming that irrigation occupies

almost the entire surface of the electrode. Due to the existence of two symmetry planes, the

model only considered a quarter of the real volume. Three electrode insertion depths were tested:

0.3, 0.5 and 0.7 mm. This range is similar to that obtained from a mechanical model[11] for the

recommended contact forces for ablation of the posterior wall of the left atrium (LA), between 5

and 20 g.[3]

Computer simulations were conducted to mimic three power-duration settings: low power-moderate duration (LPMD, 25 W–20 s),[3] high power-short duration (HPSD, 50 W–6 s)[12] and very high power-very short duration (VHPVSD, 90 W–4 s).[13] The power value used in the simulations was reduced by 20% since the model did not include the entire torso.[14] The simulation data were obtained up to 90 s after RF onset to examine the extra growth of the lesion due to thermal latency.[2]

As a model of an esophageal luminal temperature probe, we considered an infrared thermal imaging probe like that manufactured by Securus Medical Group's (Cleveland, OH, USA),[3,15] allowing accurate measurements of maximum esophageal luminal temperature. The probe was modeled as a 3 mm diameter (9 Fr) solid cylinder located inside the esophagus. Tissue properties were taken from the IT'IS Foundation database,[16] while the ablation catheter properties were taken from Pérez et al.[17] We assumed that the temperature probe was mainly made of polyurethane.[18] Each model was made up of approximately 420,000 tetrahedral elements. The outer dimensions, mesh size (minimum of 20 μm around the electrode and maximum of 6 mm in the periphery) and time step (~ 60 ms) were verified by means of convergence tests. The model solved a coupled electric-thermal problem numerically using the Finite Element Method with ANSYS software (ANSYS, Canonsburg, PA, USA). Details of the governing equations and boundary conditions are described in detail elsewhere.[19]

2.2. Peak luminal esophageal temperature

Each simulation provided the temperature value at all times and at all points (Fig. 1A). The temperature map of the inner surface of the esophagus covered 360º and a vertical segment of 6 cm (Fig. 1B). The probe was assumed to be perfectly centered and aligned with the ablation

electrode, the temperature map showed a hot spot exactly in the center of the image (Fig. 1C), where the maximum temperature was the peak temperature (T_{peak}). As the computer model only represents a quarter of the real volume, when the computed temperature map is quadrupled a complete image of 360º vision and height 60 mm is obtained (see Fig. 1D) which is similar to that reported in clinical studies.[3,15] Due to thermal latency, T_{peak} is expected to continue to grow after RF termination at t_{RF} (see Fig. 2A). In order to describe its evolution, the following parameters were analyzed: 1) its value at t_{RF} (i.e. $T_{peak-20s}$ for LPMD, $T_{peak-6s}$ for HPSD and $T_{peak-4s}$ for VHPVSD), 2) reached maximum value ($T_{peak-MAX}$), which occurred a time t_{MAX} after t_{RF}, and 3) the difference between $T_{peak-MAX}$ and the value at t_{RF} (ΔT_{peak}), which represents the increment of T_{peak} during the post-RF period.

2.3. Thermal damage model

Damaged esophagus volume was computed using a method that simultaneously takes the temperature and the exposure time into account. The model's thermal equations and derivation are detailed in the Appendix. The volume of esophageal injury (V_E) was quantified as the tissue volume in which the injury index Ω was ≥ 1 at 90 s (Fig. 1E), which is equivalent to assuming as damaged tissue that in which the percentage of undamaged cells is less than 36.7% (the thick black line in Figure A1 of the Appendix represents the boundary between damaged and undamaged tissue). As a result, our model assumed that irreversible damage occurred when the percentage of destroyed cells was higher than 63.3%. The evolution of V_E was described by means of two parameters (Fig. 2B): 1) its value at t_{RF} (V_{E-20s} for standard setting, V_{E-6s} and V_{E-4s} for HPSD and VHPVSD, respectively) and 2) its value after the post-RF period (V_{E-90s}).

6

2.4. Statistics

This study used a physics-based mechanistic model. We assumed an uncertainty in the distance between esophagus and endocardium, thicknesses of the tissues in between, and electrode insertion depth, as detailed above. This provided 135 cases for each power setting (a total of 405 simulations) that could represent a representative sample of what happens during ablation of the posterior LA wall. The Supplementary material (Excel file) includes the raw data for the construction of the model and the results. The relationships between the thermally damaged esophageal volume (V_E) and other variables (including T_{peak}) were studied by simple regression (linear or exponential).

3. Results

3.1. Relation between peak luminal temperature and the volume of esophageal injury

Figure 3 shows the relationship between the damaged esophagus volume at 90 s and the peak temperature for each of the ablation parameters tested (LPMD, HPSD, and VHPVSD) at both the time of RF termination and when the peak temperature reached its maximum value. While there was a very close relationship between V_{E-90s} and $T_{peak-MAX}$ for any power setting ($R^2 > 0.97$), the relationship between V_{E-90s} and the temperature reached at t_{RF} was lower as the duration of ablation was reduced: 0.98 for $T_{peak-20s}$, 0.93 for $T_{peak-6s}$ and only 0.77 for $T_{peak-4s}$. The temperature thresholds above which the esophagus is damaged were similar for each ablation parameter: 46.93 ºC for LPMD, 46.44 ºC for HPSD and 46.36 ºC for VHPVSD.

For any power setting, $T_{peak-MAX}$ was strongly correlated ($R = 96$) with the depth of damage across the esophagus wall (in cases where the damage did not affect the entire wall) and with the damage area measured on the inner wall of the esophagus (in cases where damage crossed the

7

entire esophageal wall).

3.2. Growth of the volume of esophageal injury after RF termination

Figure 4 shows the relationship between the volume of esophageal injury at RF termination and the volume at the end of the post-RF period at 90 s. The results show that the volume of esophageal injury notably increased after t_{RF} for any power setting, and that the damaged esophagus volume at 90 s was overall larger with LPMD (up to 81 mm^3) than with HPSD and VHPVSD (up to 32–35 mm^3). With LPMD there was a very high correlation ($R^2 = 0.97$) between both volumes (Fig. 4A). V_{E-90s} grows by approximately 50% during the post-RF period. In the HPSD and VHPVSD cases, lesion growth was overall more pronounced than for standard setting, with V_{E-90s} growing by ~240% and 270% respectively following the termination of RF.

3.3. Peak luminal temperature dynamics during post-RF period

Figure 5 shows the relationship between peak temperature at RF termination and its evolution during the post-RF period, specifically its maximum increase (ΔT_{peak}) and the delay with which it occurs (t_{MAX}). The ΔT_{peak} was greater as the RF pulse was shorter: 0.5–3.5 ℃ for LPMD, 1.4–8.5 ℃ for HPSD and 1.7–11.0 ℃ for VHPVSD (Fig. 5D–F). The maximum value of ΔT_{peak} occurred regardless of power setting in those cases in which the temperature at t_{RF} was in the approximate range 42–47 ℃. The lowest values of ΔT_{peak} corresponded with cases in which the temperature at t_{RF} was either very low (~37 ℃) or very high (> 47 ℃).

The time until reaching maximum T_{peak} was closely related to the temperature reached at t_{RF} for any power setting (Fig. 5A–C), with correlation coefficients of 0.95 for LPMD, 0.77 for HPSD and 0.76 for VHPVSD. The lower the T_{peak} value at t_{RF}, the later the maximum value is

reached. The ranges of t_{MAX} were overall similar for the three power settings: 2–42 s for standard setting, 8–48 s for 50 W–6 s and 6–48 s for 90 W–4 s.

The relationship between the endocardium-esophagus distance and T_{peak} dynamics during the post-RF period is demonstrated in Figure 6. For each power setting we found a close linear relationship ($R^2 > 0.92$) between t_{MAX} and the endocardium-esophagus distance: the greater the distance, the longer it takes T_{peak} to reach its maximum value; from 2–15 s for 2.5 mm to 42–48 s for 7 mm (Fig. 6A–C). For the relationship between ΔT_{peak} and the endocardium-esophagus distance, we found a large dispersion in the case of LPMD with a nonlinear relationship with the highest value of ΔT_{peak} (up to ~3.5 ºC) occurring at intermediate distances (~5 mm), while for very long distances (7 mm) was ~2 ºC, and for very short distances (2.5 mm) it ranged from 0.5 to 2.5 ºC. In contrast, a close exponential decay relationship between ΔT_{peak} and the endocardium-esophagus distance was found in HPSD and VHPVSD cases ($R^2 = 0.92$ for 50 W–6 s and $R^2 = 0.95$ for 90 W–4 s), with ΔT_{peak} values much greater for short distances (up to 8.5 ºC for 2.5 mm) than for long ones (less than 2 ºC for 7 mm).

3.4. Anatomical and procedural effects on damaged esophagus volume

Figure 7 shows the relationship between V_{E-90s} and anatomical and procedural parameters. Fig. 7A–C shows that there is a slight relationship between V_{E-90s} and the endocardium-esophagus distance, but the linear fit provides low values of R^2 (< 0.62). The results do suggest that there should be no esophageal damage in the case of distances > 4.5 mm with LPMD, and > 3.5 mm with HPSD and VHPVSD, while for short distances there great variability in amount of esophageal damage. The results also showed that there is no discernible relationship between

9

damaged esophagus volume and epicardial fat thickness or electrode insertion depth (values of R^2 < 0.05).

4. Discussion

The main findings of our *in silico* study showed that:

1) The damaged esophagus volume was much larger with LPMD (up to 81 mm^3) than with HPSD and VHPVSD (up to 32–35 mm^3). A direct relationship between the damaged esophagus volume and the total energy applied is physically reasonable (e.g. the volume computed with VHPVSD −360 J−, was significantly larger than with HPSD −300 J− from a paired T-Test, P=0.0169);

2) Maximum peak temperature after termination of RF application is a good predictor of esophageal damage volume regardless of the power setting whether captured by infrared thermography or any system that ensures the maximum value is being accurately measured;

3) HPSD and VHPSD were associated with greater thermal latency, with relatively more heating and esophageal damage occurring after termination of RF energy than with LPMD. This thermal latency suggests that slower conductive tissue heating plays an important role for lesion growth after RF termination during both HPSD and VHPVSD, and therefore may require lower esophageal temperature cutoffs during ablation than LPMD;

4) There is an inverse relationship between damaged esophagus volume and the endocardium-esophagus distance and no damage is seen when the distance exceeds 4.5 mm for LPMD and 3.5 mm for HSPS and VHPVSD;

5) Neither the presence of epicardial fat nor the depth of insertion of the electrode were good predictors of esophageal damage.

4.1. Comparison with Clinical Data

Our conclusions are inconsistent with both Kaneshiro *et al* [6] who showed higher incidence of esophageal injury with HPSD (45–50 W) compared to standard setting (20–30 W, 10–30 s), and Baher *et al* [20] who showed similar incidence of esophageal injury between HPSD (50 W – 5 s) and low-power long-duration (≤35 W for 10–30 s). Unlike studies based on computational modeling, in clinical ablations it can be difficult to control for a number or parameters. For example, in the study of Kaneshiro *et al* the total energy with the standard setting could have varied significantly from 200 J (20 W × 10 s) to 900 J (30 W × 30 s).[6] Likewise, with HPSD the duration was determined by the Ablation Index (AI) which was not modeled by us. Furthermore, Kaneshiro *et al* employed a cut-off of 41 ℃ (and a cut-off of 50 ℃ for Baher *et al*), which could provoke more damage in the case of HPSD due to thermal latency according our results.

Clinical data on the dynamics of T_{peak} are not abundant, especially for HPSD. The maximum value of T_{peak} computed for the LPMD (63.5 ℃) was comparable with the maximum values reported using infrared imaging as modeled in our previous work (66 ℃,[15] 65 ℃ [3]). In the case of HPSD, although there is no clinical data using infrared imaging, we can compare with the data provided by Barbhaiya *et al* [12] who used a 12-point esophageal temperature monitor (CIRCA S-CATH, Circa Scientific, Englewood, CO, USA). Despite the small sample size (16 patients), their results showed a relationship (with poor correlation, $R^2 \sim 0.40$) between ΔT_{peak} and the 'lesion-sensor' distance that is qualitatively very similar to our relationship between ΔT_{peak} and endocardium-esophageal distance. They reported a maximum value of ΔT_{peak} of 5.8 ℃ for

'lesion-sensor' distances ≤ 5 mm, which is within the range obtained by us (3.5−8.5 ℃) for those same distances. They also observed a marked effect of thermal latency, with values of t_{MAX} between 11 and 34 s, which fits our range quite well (8−48 ℃).

We did not find a close relationship between esophageal lesion volume and insertion depth of the electrode. This seems to contradict the clinical results that do show a reduction in esophageal damage for low contact forces (<20 g).[21] However, the reason could be that our model only considered moderate insertion depths (0.3−0.7 mm, see methods), thus not contemplating cases of high contact forces (>20 g) which would possibly be associated with depths greater than 0.7 mm.

4.2. Peak luminal temperature and damaged esophagus volume

When we analyzed only those simulations in which the T_{peak} at t_{RF} was 41−42 ℃ (which could mimic RFCA with cut-off temperature), we observed that LPMD did not cause damage to the esophagus ($V_{E-90s} = 0$ mm^3) and that $T_{peak-MAX}$ reached 44.3 ± 0.5 ℃ (n=13 cases). In contrast, HPSD did provoke a V_{E-90s} of 2.9 ± 2.8 mm^3 with $T_{peak-MAX}$ reached 47.3 ± 1.1 ℃ (n=5 cases), and VHPVSD also provoked a V_{E-90s} of 11.3 ± 6.7 mm^3 with $T_{peak-MAX}$ reached 50.0 ± 2.0 ℃ (n=10 cases). This analysis suggests that using the same cut-off value for LPMD and HPSD/VHPVSD may not be safe.

4.3. Growth of volume of esophageal injury after RF termination

Two important observations regarding the increase in the volume of esophageal injury after RF termination are noteworthy: 1) there was a relatively high increase of T_{peak} after RF termination, up to 3.5 ℃ for LPMD s and up to 11 ℃ for VHPVSD s, and 2) the T_{peak} reaches the maximum

12

values after a relatively long time and independent of the power setting, and there was more delay to the maximum temperature with a lower lower T_{peak} at RF termination.

If we focus exclusively on those cases with esophageal injury ($V_{E-90s} > 0$ mm^3), which correspond with endocardium-esophagus distances < 5 mm for LPMD and < 4 mm for HPSD and VHPVSD, our results highlight which cases the evolution of T_{peak} during the post-RF period could be causing esophageal injury. In particular, in the case of LPMD, esophagus injury could be suspected when T_{peak} increases between 0.5 and 3.5 ºC within the first 25 s of the post-RF period In the case of HPSD and VHPVSD, esophagus injury could be suspected when T_{peak} increases between 4.5 and 8.5 ºC within the first 25 s of the post-RF period.

While our results confirm that there is an inverse relationship between damaged esophagus volume and the endocardium-esophagus distance, there is a higher variability in esophageal damage as the endocardium-esophagus distance is shorter. Since the RF power is distributed in a narrow area (1−2 mm) around the electrode, heating in the esophagus will be more influenced by the RF energy deposition itself with a shorter endocardium-esophagus distance. As this deposition is strongly influenced by the conditions close to the electrode ('local environment'), such as the insertion depth of the electrode and electrical conductivity of the nearest tissue (including the presence or absence of epicardial fat), it seems reasonable to assume that the variation of these factors will have a much greater impact on the volume of damaged esophagus when the esophagus is close to the electrode.

No other anatomical factors such as the presence of epicardial fat or the depth of insertion of the electrode could reliably predict esophageal damage in our model.

4.4. Clinical implications

13

The computational model results presented in this study suggest that even in the case of standard settings, thermal latency can play a relevant role during the post-RF period which can cause further esophageal injury that is directly proportional related to the increase in esophageal temperature that the electrophysiologist may observe in the seconds following cessation of RF power. The most probable cases of esophageal injury would be those in which an increase of T_{peak} during the post-RF period occurs in the first 25 s. Interestingly, in the case of standard settings, a small increase of T_{peak} (e.g. only 0.5 ºC) would not necessarily suggest less injury than a larger increment of up to 3.5 ºC. In contrast, in the case of HPSD and VHPVSD, greater increases in T_{peak} would be required for a significant amount of esophageal injury. Using the canine thigh muscle preparation, Nakagawa et al recently showed that most of the effective tissue heating and lesion formation in VHPVSD (90W-4s) RF applications occurs after RF termination due to conductive tissue heating (i.e., thermal latency).[22]

Although monitoring T_{peak} in order to stop the application of RF seems safe and effective with LPMD, its use with HPSD and VHPVSD could be limited due to the slightly lower correlation between T_{peak} and the damaged esophagus volume. Since electrode-esophagus distance seems to be the most relevant parameter affecting the damaged esophagus volume, a safe strategy to decrease the injury would to lower the total applied RF energy as much as possible in the case of ablations close to the esophagus (e.g. using HPSD instead of standard setting).[12,13]

4.5. Limitations

Our model was aimed to to assess the amount of esophagus tissue thermally affected by ablation, and it did not take hence into account the cellular mechanisms that lead to creation of fistulas. Another important limitation is that it only considered the RF catheter in a vertical position, even though other positions are possibly more common in left atrial posterior wall ablation. In this

14

regard, although the results in quantitative terms could be different for a parallel or 45º angle, there is no physical reason to suspect that the conclusions would not be valid in terms of the relationship between peak temperature, thermal latency and volume of damaged esophagus.

This study has also several limitations related with the modeling technique. First, blood flow and electrode irrigation were modeled in a simplified way as described in González-Suárez *et al*,[23] i.e. without solving the fluid dynamics. Although this approach fails when predicting the surface width of the thermal lesion, it is able to predict the lesion depth, which is the dimension relevant to our aim of estimating the thermally damaged esophageal volume. Moreover, since the approach to modeling the irrigation was that of a multi-hole irrigation-tip electrode, we must recognize that slightly different results could be obtained with another type of irrigation (such as one based on a small number of holes).

Secondly, the mechanical deformation of the endocardial surface was not modeled,[11] which would possibly alter the absolute values of lesion depth obtained, but not the study's conclusions. Thirdly, the model did not include the motion effect of heartbeats or breathing. Despite the fact that both factors produce clearly observable variations in the contact force (CF) as measured by some catheters,[24] a recent *in silico* study including heartbeat-induced electrode displacement (CF ranging from 10 to 30 g) showed hardly any differences in lesion size (<0.04 mm) compared to a model that did not include these effects.[25] For this reason we do not think that these factors would invalidate our conclusions. It should be pointed out that we only modeled low value cases (<20 g) and the results thus could be different for higher values.

Fourthly, we did not consider multi-parametric indexes such as Ablation Index (AI)[26] and Lesion Index (LSI)[27] to guide RFCA. Although the indexes are clinically associated with more successful with fewer complications, they are really manufacturer-dependent indexes based on complex formulas not easily understood from a physical point of view by the average user. In this

regard, our study was not intended to assess these particular indexes, but rather to improve the understanding of the physical phenomena during RFCA. We therefore considered settings based exclusively on power and time, two easily understandable physical variables. Interestingly, *in silico* models like the one used in our study could be used as a complementary tool to assess RF ablations guided by this type of index.

Finally, note that our model assumed the esophageal temperature probe to be optimally placed respect the ablation site. While we we recognized that the relation between the positioning of the RF electrode and the thermal probe is crucial, this issue has been already addressed in a previous computer model.[28] In light of that study, it seems reasonable to assume that any deviation of the probe from its optimal location will imply an underestimation of the temperature measurement.

5. Conclusions

In this computer anatomic model of esophageal temperature rise using standard ablation settings and HPSD, we demonstrate that peak temperature and the volume of injured esophageal tissue over time differ between LPMD and HPSD RF delivery. As visually summarized in Fig. 8, while the total V_E was highest in the LPMD under otherwise similar conditions, the HPSD and VHPVSD cases showed more significant thermal latency and therefore maximum risk for esophageal temperature occurring later after cessation of RF application.

APPENDIX

Thermal damage model and derivation

We used the injury index Ω based on the Arrhenius' experimental observations in the 1880s, which relates the number of undamaged cells $C(0)$ present before the heating to the remaining number of undamaged cells at time τ indicated by $C(\tau)$ as follows:

$$\Omega(\tau) = \ln(\frac{C(o)}{C(\tau)}) \tag{1}$$

It can be computed from the 'thermal history' to which the tissue is subjected, specifically from the temperature T (in Kelvin) reached at each instant t (s) of the heating period:

$$\Omega(\tau) = \int_0^\tau A e^{[-E_a/RT(t)]} dt \tag{2}$$

where A is the frequency factor (1/s), E_a is the activation energy (J/mol), and R the universal gas constant (8.3143 J/mol·K). The values of A and E_a are particular for each tissue type and analyzed process. In the past we reported the histological changes in rabbit esophagus subjected to heating with different temperature–duration combinations.[28] We now have analyzed the adequacy of the values of A and E_a previously used for *ex vivo* liver: $7.39 \cdot 10^{39}$ s^{-1} and $2.577 \cdot 10^5$ J/mol, respectively.[17] For that, we compared the remaining number of undamaged cells $C(\tau)$ computed using Equation (1) and (2) to the histological findings reported in Lequerica *et al.*[29] The results are shown in Figure A1.

References

1. Wittkampf FH, Nakagawa H, Yamanashi WS, et al. Thermal latency in radiofrequency ablation. Circulation. 1996 Mar 15;93(6):1083-6. doi: 10.1161/01.cir.93.6.1083.
2. Irastorza RM, d'Avila A, Berjano E. Thermal latency adds to lesion depth after application of high-power short-duration radiofrequency energy: Results of a computer-modeling study. J Cardiovasc Electrophysiol. 2018 Feb;29(2):322-327. doi: 10.1111/jce.13363.
3. Deneke T, Nentwich K, Berkovitz A, et al. High-resolution infrared thermal imaging of the esophagus during atrial fibrillation ablation as a predictor of endoscopically detected thermal lesions: results from the HEAT-AF study. Circ Arrhythm Electrophysiol. 2018 Nov;11(11):e006681. doi: 10.1161/CIRCEP.118.006681.
4. Bourier F, Duchateau J, Vlachos K, et al. High-power short-duration versus standard radiofrequency ablation: Insights on lesion metrics. J Cardiovasc Electrophysiol. 2018 Nov;29(11):1570-1575. doi: 10.1111/jce.13724.
5. Leshem E, Zilberman I, Tschabrunn CM, et al. High-Power and Short-Duration Ablation for Pulmonary Vein Isolation: Biophysical Characterization. JACC Clin Electrophysiol. 2018 Apr;4(4):467-479. doi: 10.1016/j.jacep.2017.11.018.
6. Kaneshiro T, Kamioka M, Hijioka N, et al. Characteristics of Esophageal Injury in Ablation of Atrial Fibrillation Using a High-Power Short-Duration Setting. Circ Arrhythm Electrophysiol. 2020 Oct;13(10):e008602. doi: 10.1161/CIRCEP.120.008602.
7. Berjano EJ, Hornero F. What affects esophageal injury during radiofrequency ablation of the left atrium? An engineering study based on finite-element analysis. Physiol Meas. 2005 Oct;26(5):837-48. doi: 10.1088/0967-3334/26/5/020.
8. Sánchez-Quintana D, López-Mínguez JR, Macías Y, et al. Left atrial anatomy relevant to catheter ablation. Cardiol Res Pract. 2014;2014:289720. doi: 10.1155/2014/289720.
9. Ho SY, Cabrera JA, Sánchez-Quintana D. Vagaries of the vagus nerve: relevance to ablationists. J Cardiovasc Electrophysiol. 2006 Mar;17(3):330-1. doi: 10.1111/j.1540-8167.2006.00364.x.
10. Pérez JJ, D'Avila A, Aryana A, Berjano E. Electrical and thermal effects of esophageal temperature probes on radiofrequency catheter ablation of atrial fibrillation: results from a computational modeling study. J Cardiovasc Electrophysiol. 2015 May;26(5):556-64. doi: 10.1111/jce.12630. Epub 2015 Mar 27.
11. Yan S, Gu K, Wu X, et al. Computer simulation study on the effect of electrode-tissue contact force on thermal lesion size in cardiac radiofrequency ablation. Int J Hyperthermia. 2020;37(1):37-48. doi: 10.1080/02656736.2019.1708482.
12. Barbhaiya CR, Kogan EV, Jankelson L, et al. Esophageal temperature dynamics during high-power short-duration posterior wall ablation. Heart Rhythm. 2020 May;17(5 Pt A):721-727. doi: 10.1016/j.hrthm.2020.01.014.
13. Kotadia ID, Williams SE, O'Neill M. High-power, Short-duration Radiofrequency Ablation for the Treatment of AF. Arrhythm Electrophysiol Rev. 2020 Feb 12;8(4):265-272. doi: 10.15420/aer.2019.09.
14. Irastorza RM, Gonzalez-Suarez A, Pérez JJ, et al. Differences in applied electrical power between full thorax models and limited-domain models for RF cardiac ablation. Int J Hyperthermia. 2020;37(1):677-687. doi: 10.1080/02656736.2020.1777330.
15. Daly MG, Melton I, Roper G, et al. High-resolution infrared thermography of esophageal temperature during radiofrequency ablation of atrial fibrillation. Circ Arrhythm Electrophysiol. 2018 Feb;11(2):e005667. doi: 10.1161/CIRCEP.117.005667..
16. Hasgall PA, Di Gennaro F, Baumgartner C, et al, "IT'IS Database for thermal and electromagnetic parameters of biological tissues," Version 4.0, May 15, 2018, DOI: 10.13099/VIP21000-04-0. itis.swiss/database.
17. Pérez JJ, Ewertowska E, Berjano E. Computer modeling for radiofrequency bipolar ablation inside ducts and vessels: relation between pullback speed and impedance progress. Lasers Surg Med. 2020 Nov;52(9):897-906. doi: 10.1002/lsm.23230.
18. Garibotto JT, Auger SR, Flaherty RM, et al. Temperature measurement systems, method and devices. US Patent 2020/0214573 A1 (Jul 9, 2020).
19. Pérez JJ, González-Suárez A, Berjano E. Numerical analysis of thermal impact of intramyocardial capillary blood flow during radiofrequency cardiac ablation. Int J Hyperthermia. 2018 May;34(3):243-249. doi: 10.1080/02656736.2017.1336258.
20. Baher A, Kheirkhahan M, Rechenmacher SJ, et al. High-Power Radiofrequency Catheter Ablation of Atrial Fibrillation: Using Late Gadolinium Enhancement Magnetic Resonance Imaging as a Novel Index of Esophageal Injury. JACC Clin Electrophysiol. 2018 Dec;4(12):1583-1594. doi: 10.1016/j.jacep.2018.07.017.

21. Zhang X, Kuang X, Gao X, Xiang H, Wei F, Liu T, Wu H, Wang G, Zuo Z, Wang L, Ding L, Zhang J, Shehata M, Wang X, Yang B, Fan J. RESCUE-AF in Patients Undergoing Atrial Fibrillation Ablation: The RESCUE-AF Trial. Circ Arrhythm Electrophysiol. 2019 May;12(5):e007044. doi: 10.1161/CIRCEP.118.007044.

22. Nakagawa H, Ikeda A, Sharma T, Govari A, Ashton J, Maffre J, Lifshitz A, Fuimaono K, Yokoyama K, Wittkampf FHM, Jackman WM. Comparison of In Vivo Tissue Temperature Profile and Lesion Geometry for Radiofrequency Ablation With High Power-Short Duration and Moderate Power-Moderate Duration: Effects of Thermal Latency and Contact Force on Lesion Formation. Circ Arrhythm Electrophysiol. 2021 Jul;14(7):e009899. doi: 10.1161/CIRCEP.121.009899. Epub 2021 Jun 17. PMID: 34138641.

23. González-Suárez A, Pérez JJ, Berjano E. Should fluid dynamics be included in computer models of RF cardiac ablation by irrigated-tip electrodes? Biomed Eng Online. 2018 Apr 20;17(1):43. doi: 10.1186/s12938-018-0475-7.

24. Sarkozy A, Shah D, Saenen J, Sieira J, Phlips T, Boris W, Namdar M, Vrints C. Contact Force in Atrial Fibrillation: Role of Atrial Rhythm and Ventricular Contractions: Co-Force Atrial Fibrillation Study. Circ Arrhythm Electrophysiol. 2015 Dec;8(6):1342-50. doi: 10.1161/CIRCEP.115.003041.

25. Pérez JJ, González-Suárez A, Berjano E. Computer modeling of radiofrequency cardiac ablation including heartbeat-induced electrode displacement. Under review in *Computer Methods and Programs in Biomedicine.*

26. Das M, Loveday JJ, Wynn GJ, Gomes S, Saeed Y, Bonnett LJ, Waktare JEP, Todd DM, Hall MCS, Snowdon RL, Modi S, Gupta D. Ablation index, a novel marker of ablation lesion quality: prediction of pulmonary vein reconnection at repeat electrophysiology study and regional differences in target values. Europace. 2017 May 1;19(5):775-783. doi: 10.1093/europace/euw105. PMID: 27247002.

27. Mattia L, Crosato M, Indiani S, Causin E, Licciardello C, Maria Squasi PA, De Leo A, Calzolari V. Prospective Evaluation of Lesion Index-Guided Pulmonary Vein Isolation Technique in Patients with Paroxysmal Atrial Fibrillation: 1-year Follow-Up. J Atr Fibrillation. 2018 Apr 30;10(6):1858. doi: 10.4022/jafib.1858. PMID: 29988268; PMCID: PMC6009787.

28. Hornero F, Berjano EJ. Esophageal temperature during radiofrequency-catheter ablation of left atrium: a three-dimensional computer modeling study. J Cardiovasc Electrophysiol. 2006 Apr;17(4):405-10. doi: 10.1111/j.1540-8167.2006.00404.x.

29. Lequerica JL, Sanz E, Hornero F, et al. Esophagus histological analysis after hyperthermia-induced injury: implications for cardiac ablation. Int J Hyperthermia. 2009 Mar;25(2):150-9. doi: 10.1080/02656730802537626.
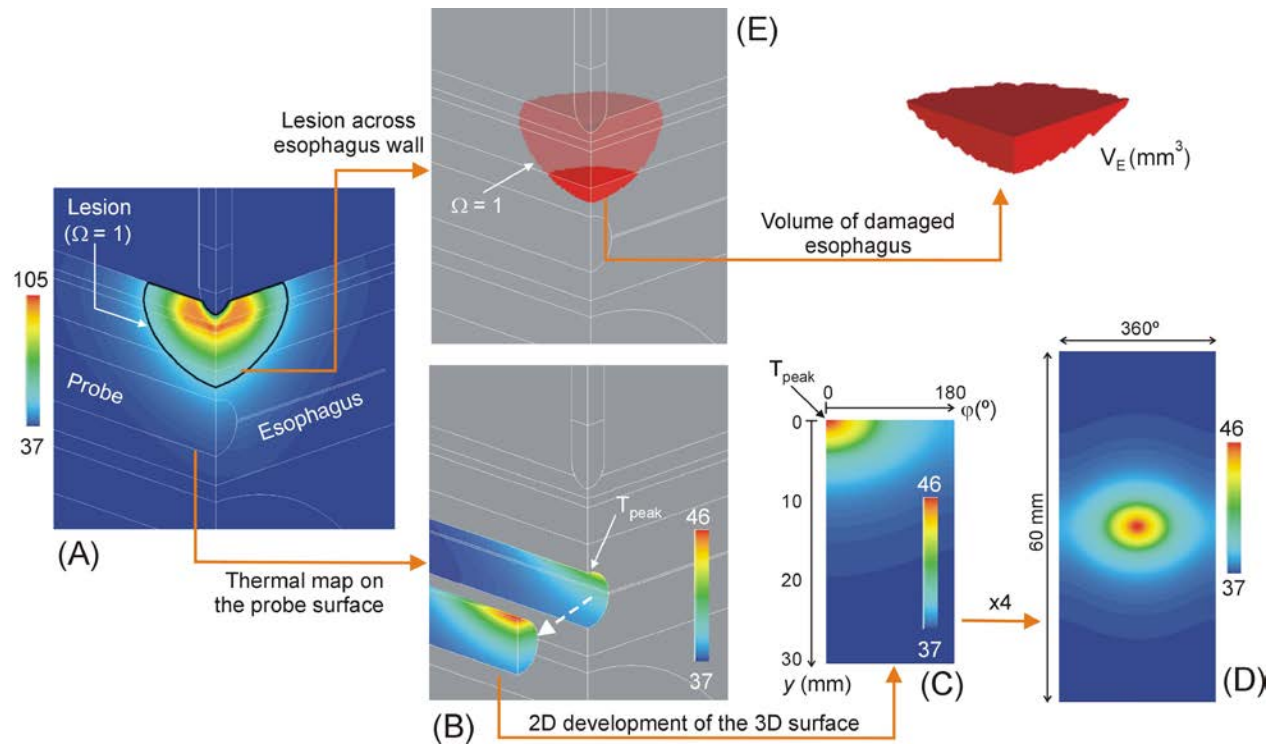
Figure 1 Graphic summary of processing of simulation results. Each simulation provided the temperature distribution in the entire model (scale in °C): **(A)** from the temperature map of the inner esophagus surface was analyzed to obtain T_{peak} **(B,C)**. T_{peak} is located in the center of the thermal image **(D)**, which is similar to those reported in clinical studies.[3,15] The temperature progress in the esophagus was used to calculate the volume of thermally damaged esophageal tissue (V_E) using the Arrhenius damage model **(E)**.
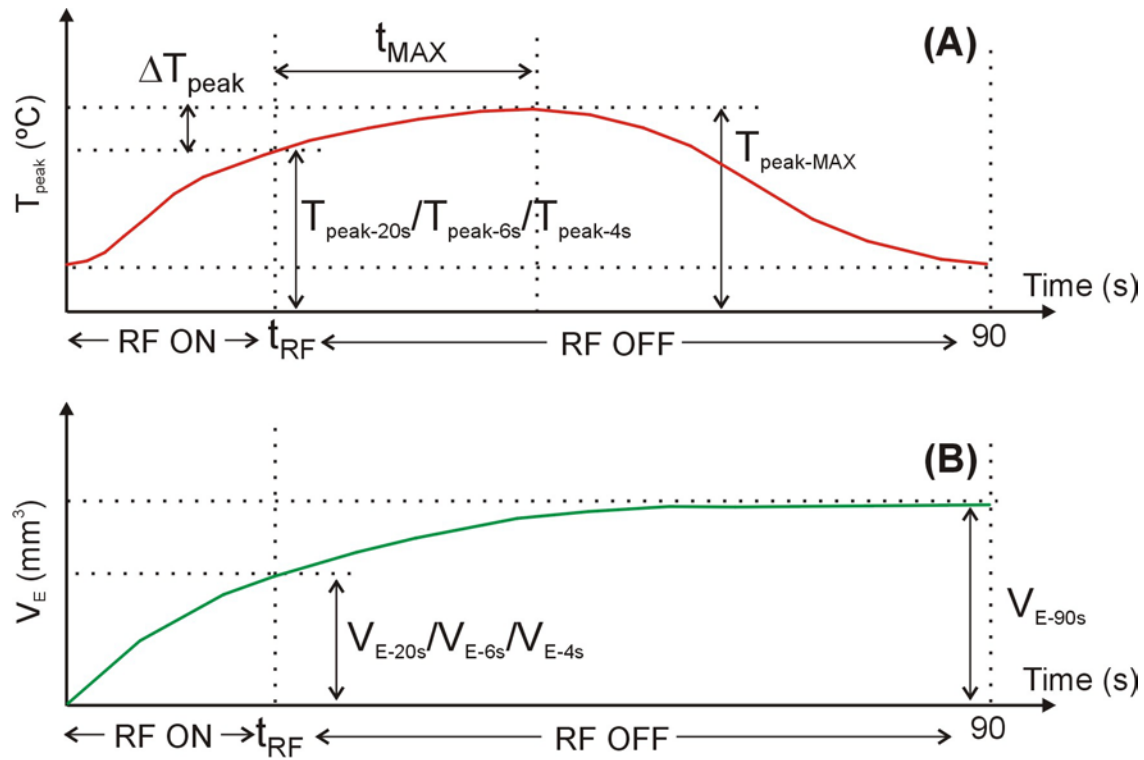
Figure 2   Relevant parameters used to characterize the evolution of the peak temperature (T_{peak})

(A) and the volume of esophageal injury (V_E) (B) during RF application t_{RF} (25 W

-20 s, 50 W $- 6$ s, 90 W $- 4$ s) and after RF termination (up to 90 s).
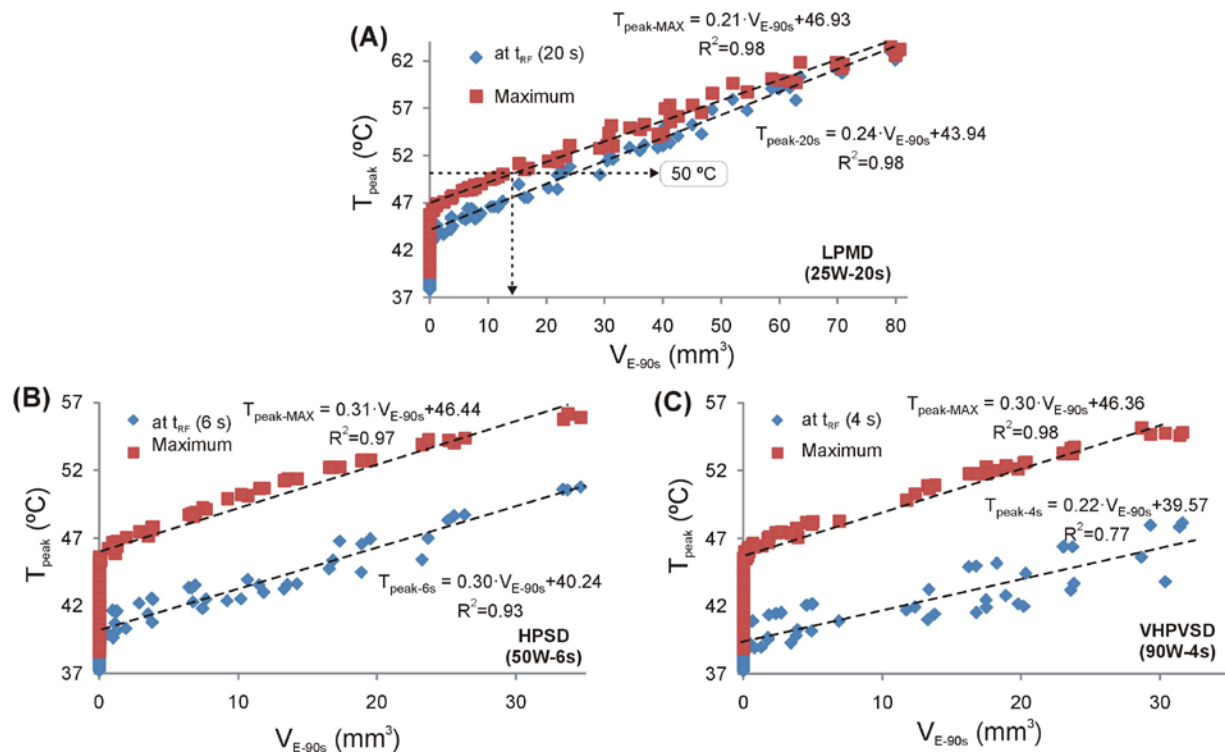
Figure 3 Relationship between the damaged esophagus volume (V_{E-90s}) and the peak luminal temperature (T_{peak}) for three power-duration settings: Low power-moderate duration, LPMD (**A**) and high-power short-duration, HPSD (**B**), and very high power-very short duration, VHPVSD(**C**). T_{peak} was computed for two different instants: at the RF termination (i.e. $T_{peak-20s}$ for LPMD, $T_{peak-6s}$ for HPSD and $T_{peak-4s}$ for VHPVSD), and when it reaches the maximum value several seconds later ($T_{peak-MAX}$). Cases with no damage ($V_{E-90s} = 0$ mm^3) were omitted for the regression analyses.
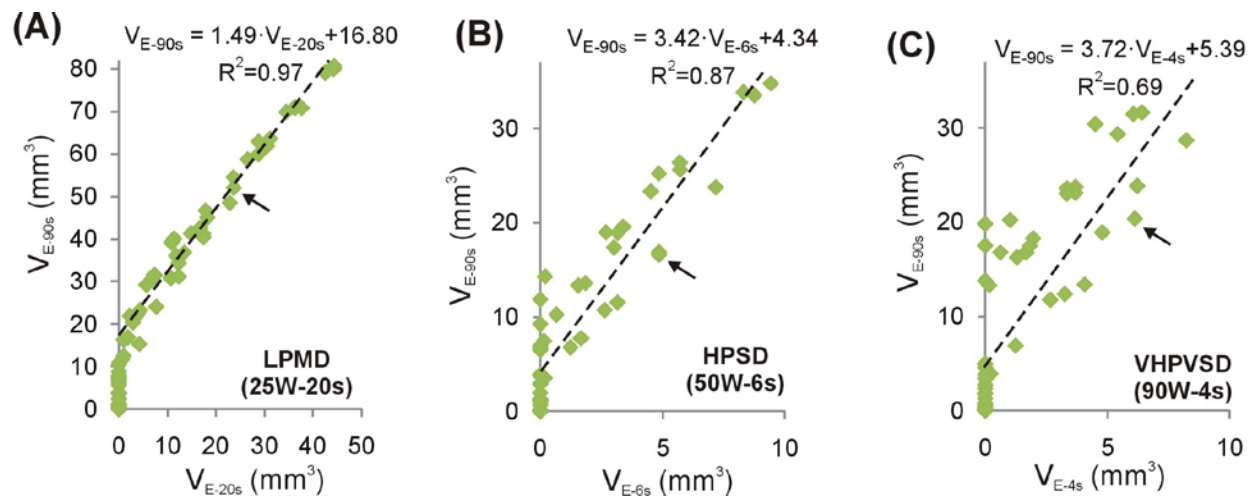
Figure 4 Relationship between the volume of esophageal injury after RF termination (V_{E-90s}) and the volume of esophageal injury at the RF termination (V_{E-20s} for LPMD **(A)**, V_{E-6s} for HPSD **(B)** and V_{E-6s} for VHPVSD **(C)**. Cases with no damage ($V_{E-90s} = 0$ mm^3) were omitted for the regression analyses. The arrows indicate the specific case plotted in Fig. 8.
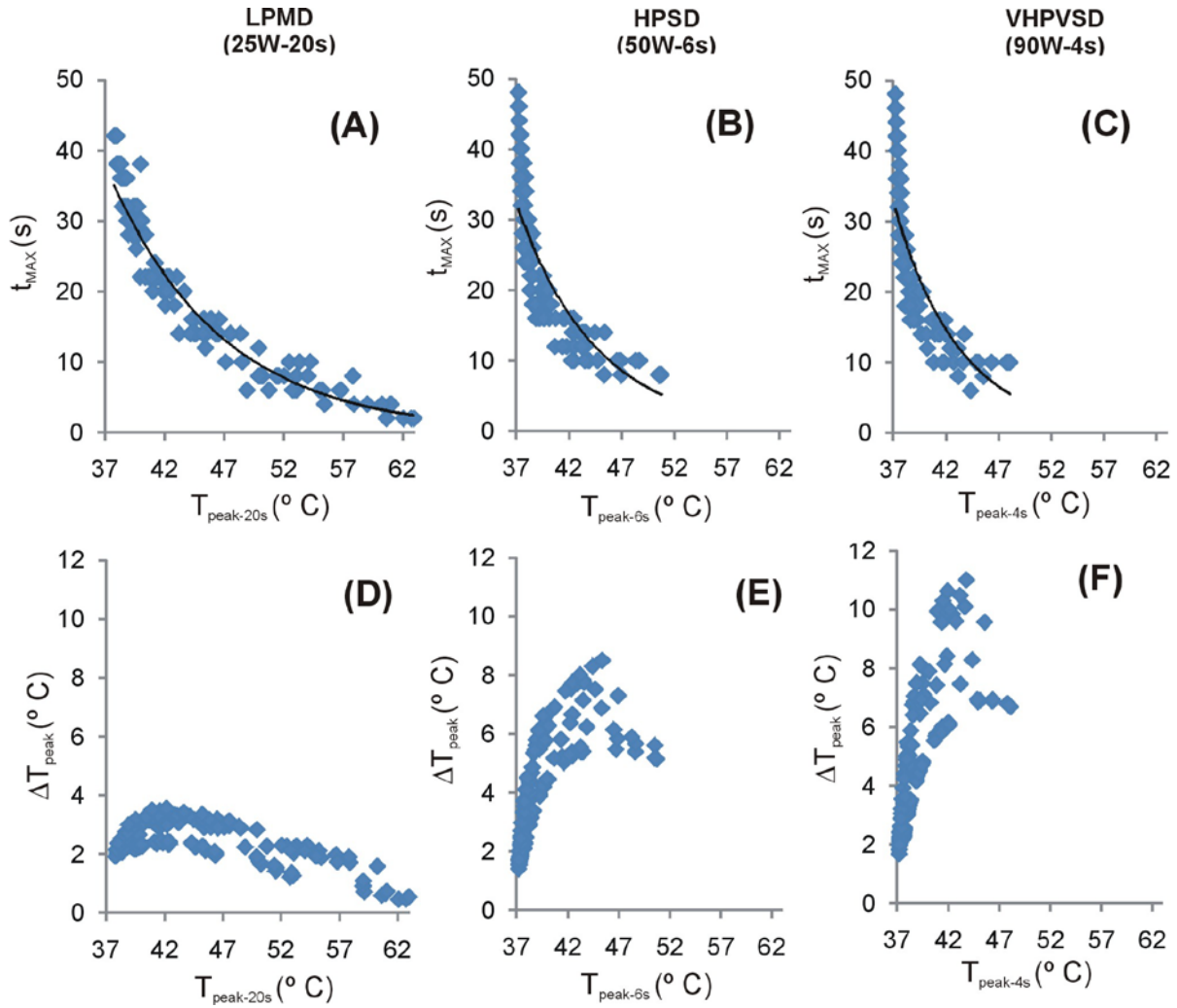
Figure 5   Relationship between the peak luminal temperature (T_{peak}) at the RF termination (i.e. $T_{peak-20s}$ for LPMD, $T_{peak-6s}$ for HPSD and $T_{peak-4s}$ for VHPVSD) and the T_{peak} dynamics after RF termination, specifically with the time that passes from RF termination until T_{peak} reaches its maximum value (t_{MAX}) **(A–C)** and with ΔT_{peak} (temperature increase occurring after RF termination) **(D–F)**.
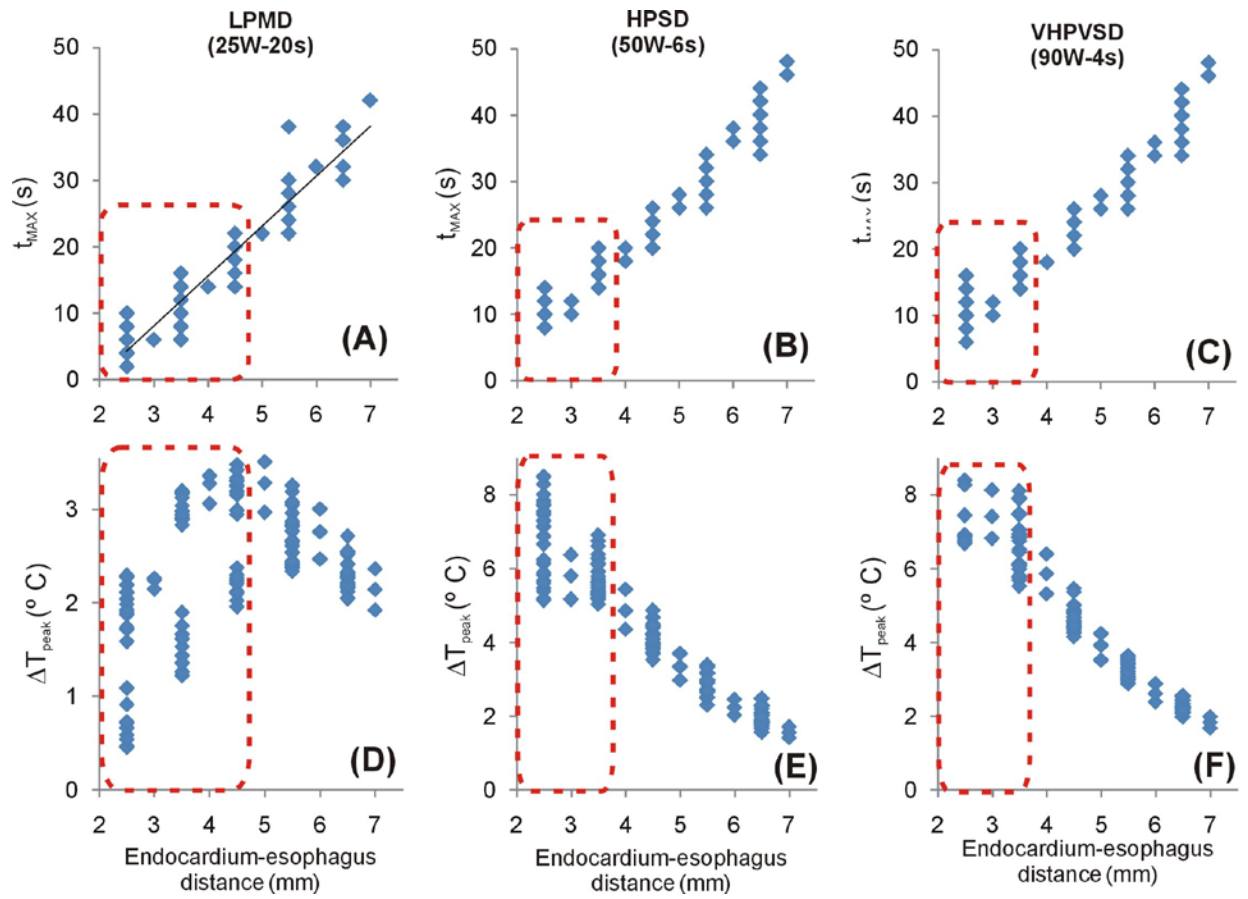
Figure 6 Relationship between t_{MAX} (time that passes from when the RF power ceases until T_{peak} reaches its maximum value) and the endocardium-esophagus distance for LPMD (**A**), HPSD (**B**) and VHPVSD (**C**). Relationship between ΔT_{peak} and the endocardium-esophagus distance for LPMD (**D**), HPSD (**E**) and VHPVSD (**F**). The rectangles group the cases where there is esophageal injury, i.e. $V_{E-90s} > 0$ mm^3.
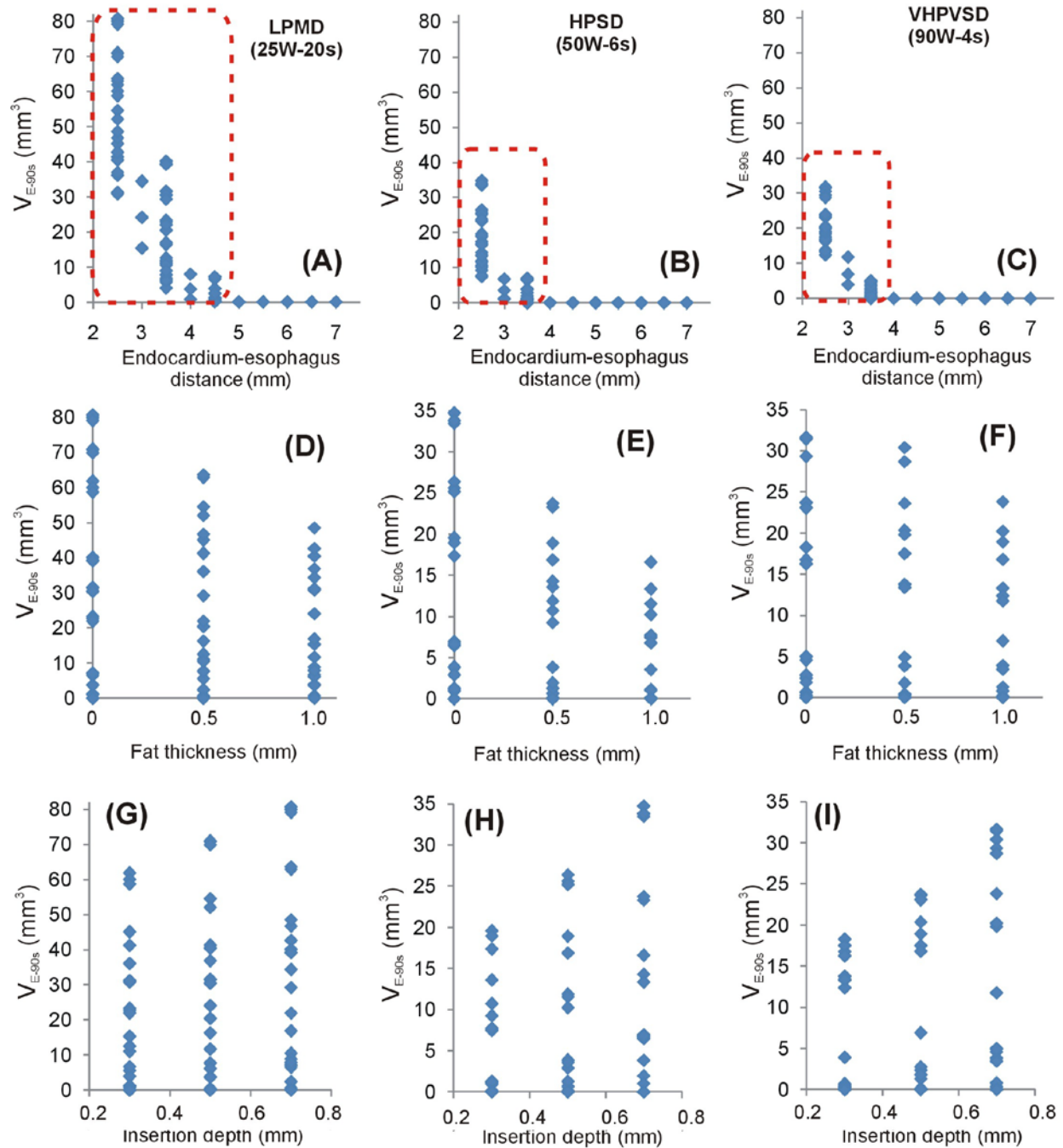
Figure 7 Relationship between the volume of esophageal injury after RF termination (V_{E-90s}) and endocardium-esophagus distance **(A−C)**, epicardial fat layer thickness **(D−F)** and insertion depth of the electrode into the tissue **(G−I)** for the three power settings (LPMD, HPSD, VHPVSD).
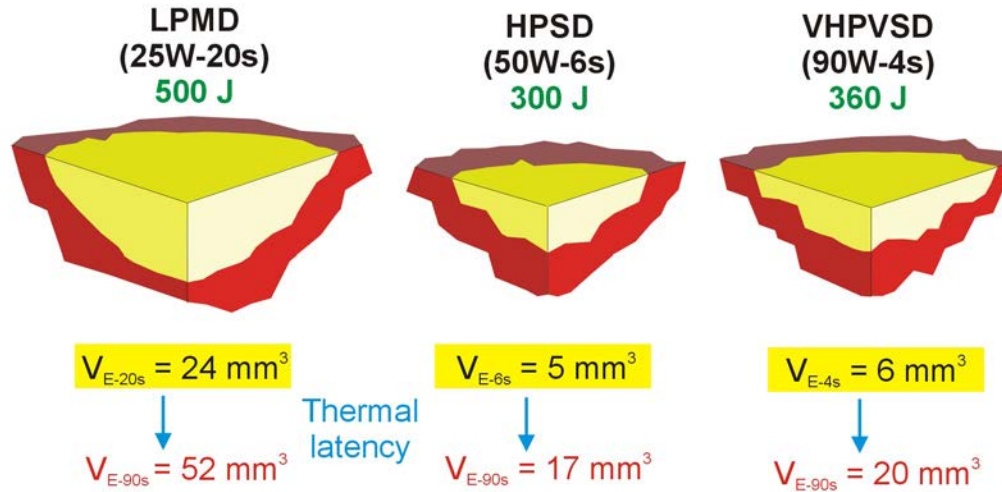
Figure 8 Volume of thermally damaged esophageal tissue (V_E) for the three power settings (LPMD, HPSD, VHPVSD). The yellow volume represents the damaged tissue just after the RF pulse ceases and the red volume is the growth that occurs during the RF-post period of 90 s. V_E is greater with LPMD (as expected due to higher energy distributed (500 J vs. 300 and 360 J). However, the cases of HPSD and VHPVSD show a more significant thermal latency, i.e. a greater growth of V_E during the post-RF period. The three plots correspond to the specific case of 0.5 mm electrode insertion, 2 mm atrial wall, 0.5 mm fat layer, 0 mm connective tissue, i.e. 2.5 mm endocardium-esophagus distance (highlighted in Fig. 4).

		Temperature (ºC)							
		40		50		60		70	
Time (s)	30	o	98% (0)	o	63% (0.5)	+++	0% (8.3)	+++	0% (126)
	60	o	96% (0)	+	39% (0.9)	+++	0% (17)	+++	0% (252)
	90	o	94% (0.1)	++	25% (1.4)	+++	0% (25)	+++	0% (378)

Figure A1. Comparison between the subjective levels of thermal damage from the histological analysis (o, +, ++, +++) and the remaining percentage of undamaged cells $C(\tau)$ computed using the Arrhenius method (see Equations (1) and (2)). The value of injury index Ω is also indicated in parentheses. Subjective level of thermal damage in the esophagus from the analysis of histological findings: o (no damage), + (light), ++ (moderate) and +++ (severe).